

### III. 研究成果に関する一覧表

研究成果の刊行に関する一覧表

書籍

著者氏名	論文タイトル名	書籍全体の編集者名	書籍名	出版社名	出版地	出版年	ページ
西村理行、齋藤正寛、波多賢二、米田俊之	分子生物硬組織研究のイノベーション	米田俊之	生命歯科医学のカッティング・エッジ	大阪大学出版会	大阪	2008	2-19

雑誌

発表者氏名	論文タイトル名	発表誌名	巻号	ページ	出版年
K. Yoshizaki, S. Yamamoto, A. Yamada, K. Yuasa, T. Iwamoto, E. Fukumoto., H. Harada, <u>M. Saito</u> , A. Nakasima, K. Nonaka, Y. Yamada, and S. Fukumoto.	Neurotrophic factor NT-4 regulates ameloblastin expression via full-length TrkB.	J Biol Chem	283	3385-3391	2008
S. Tsuchiya, M. Honda, Y. Shinohara, <u>M. Saito</u> , M. Ueda.	Collagen type I matrix affects the molecular and cellular beha	Cell Tissue Res	331	447-459	2008
M. Shiga, <u>M. Saito</u> , M. Hattori, C.Torii K. Kosaki, T. Kiyono, and N. Suda.	Characteristic phenotype of immortalized periodontal cells isolated from a Marfan syndrome type I patient	Cell Tissue Res	331	461-464	2008
E. Nishida, T. Sasaki, S. Kazuko Ishikawa, K. Kosaka, M. Aino, T. Noguchi, T. Teranaka, N. Shimizu and <u>M. Saito</u> .	Transcriptome Database KK-Periome for Periodontal Ligament Development:Expression Profiles of the Extracellular Matrix Genes.	Gene	404	70-79	2007
E Hjiantonou, M Anayasa, P Nicolaou, I Bantounas, <u>M Saito</u> , S Iseki, JB Uney, LA Phylactou,	Twist induces reversal of myotube formation.	Differentiation	76	182-192	2007
N. Yoshiba, K. Yoshiba, A. Hosoya, <u>M. Saito</u> , T. Yokoi, T. Okiji, N. Amizuka, H. Ozawa	Association of TIMP-2 with extracellular matrix exposed to mechanical stress and its co-distribution with periostin during mouse mandible development.	Cell Tissue Res	330	133-145	2007
T. Yamashiro, L. Zheng, Y. Shitaku, <u>M. Saito</u> , T. Tsubakimoto, K. Takada, T. Takano-Yamamoto, I. Thesleff.	Wnt10a regulates dentin sialophosphoprotein mRNA expression and possibly links odontoblast differentiation and tooth morphogenesis.	Differentiation	75	452-462	2007
S. Yamada, M. Tomoeda, Y. Ozawa, Y. Terashima, S. Ikegawa, M. Saito, S. Toyosawa, <u>S. Murakami</u> .	PLAP-1/asporin: A novel negative regulator of periodontal ligament mineralization.	J. Biol. Chem	282	23070-23080	2007
Y. Shimabukuro, T. Ichikawa, Y. Terashima, T. Iwayama, H. Oohara, T. Kajikawa, R. Kobayashi, H. Terashima, M. Takedachi, M.	Basic fibroblast growth factor regulates expression of heparan sulfate in human periodontal ligament cells.	Matrix Biology	27	232-241	2008

Terakura, T. Hashikawa, S. Yamada, <b>S. Murakami.</b>					
Miyagawa Y, Okita H, Nakajima H, Horiuchi Y, Sato B, Taguchi T, Toyoda M, Katagiri YU, Fujimoto J, Hata JI, <b>Umezawa A</b> , Kiyokawa N.	Inducible expression of chimeric EWS/ETS proteins confers Ewing's family tumor-like phenotypes to human mesenchymal progenitor cells.	Mol Cell Biol.	28(7)	2125-37	2008
Yazawa T, Uesaka M, Inaoka Y, Mizutani T, Sekiguchi T, Kajitani T, Kitano T, <b>Umezawa A</b> , Miyamoto K.	Cyp11b1 is induced in the murine gonad by luteinizing hormone/ human chorionic gonadotropin and involved in the production of 11-ketotestosterone, a major fish androgen; conservation and evolution of androgen metabolic pathway.	Endocrinology	149(4)	1786-92	2008
Takeuchi M, Takeuchi K, Kohara A, Satoh M, Shioda S, Ozawa Y, Ohtani A, Morita K, Hirano T, Terai M, <b>Umezawa A</b> , Mizusawa H.	Chromosomal instability in human mesenchymal stem cells immortalized with human papilloma virus E6, E7, and hTERT genes.	In Vitro Cell Dev Biol Anim.	43(3-4)	129-38	2007
Yoshida Y, Shimomura T, Sakabe T, Ishii K, Gonda K, Matsuoka S, Watanabe Y, Takubo K, Tsuchiya H, Hoshikawa Y, Kurimasa A, Hisatome I, Uyama T, Terai M, <b>Umezawa A</b> , Shiota G.	A role of Wnt/beta-catenin signals in hepatic fate specification of human umbilical cord blood-derived mesenchymal stem cells.	Am J Physiol Gastrointest Liver Physiol.	293(5)	1089-98	2007
Sato B, Katagiri Y, Miyado K, Akutsu H, Miyashita Y, Horiuchi Y, Nakajima H, Okita H, <b>Umezawa A</b> , Hata J, Fujimoto J, Toshimori K, Kiyokawa N.	Preferential localization of SSEA-4 in interfaces between blastomeres of mouse preimplantation embryos.	Biochem Biophys Res Commun.	364	838-43	2007
Kato S, Mohri Y, Matsuo T, Ogawa E, <b>Umezawa A</b> , Okuyama R, Nishimori K.	Eye-open at birth phenotype with reduced keratinocyte motility in LGR4 null mice.	FEBS Lett.	581(24)	4685-90	2007
Hashii N, Kawasaki N, Nakajima Y, Toyoda M, Katagiri Y, Itoh S, Harazono A, <b>Umezawa A</b> , Yamaguchi T.	Study on the quality control of cell therapy products. Determination of N-glycolylneuraminic acid incorporated into human cells by nano-flow liquid chromatography/Fourier transformation ion cyclotron mass spectrometry.	J Chromatogr A.	1160(1-2)	263-9	2007
Toyoda M, Takahashi H, <b>Umezawa A</b> .	Ways for a mesenchymal stem cell to live on its own: maintaining an undifferentiated state ex vivo.	Int J Hematol.	86(1)	1-4	2007
Shimomura T, Yoshida Y, Sakabe T, Ishii K, Gonda K, Murai R, Takubo K, Tsuchiya H, Hoshikawa Y, Kurimasa A, Hisatome I, Uyama T, <b>Umezawa A</b> , Shiota G.	Hepatic differentiation of human bone marrow-derived UE7T-13 cells: Effects of cytokines and CCN family gene expression.	Hepatol Res.	37(12)	1068-79	2007
Okamoto K, Miyoshi S, Toyoda M, Hida N, Ikegami Y, Makino H, Nishiyama N, Tsuji H, Cui CH,	Working" cardiomyocytes exhibiting plateau action potentials from human placenta-derived extraembryonic	Exp Cell Res.	313(12)	2550-62	2007

Segawa K, Uyama T, Kami D, Miyado K, Asada H, Matsumoto K, Saito H, Yoshimura Y, Ogawa S, Aeba R, Yozu R, <u>Umezawa A.</u>	mesodermal cells.				
Nishiyama N, Miyoshi S, Hida N Miss, Uyama T, Okamoto K, Ikegami Y, Miyado K, Segawa K, Terai M, Sakamoto M, Ogawa S, <u>Umezawa A.</u>	The Significant Cardiomyogenic Potential of Human Umbilical Cord Blood-Derived Mesenchymal Stem Cells in Vitro.	Stem cells.	25(8)	2017-24	2007
Cui CH, Uyama T, Miyado K, Terai M, Kyo S, Kiyono T, and <u>Umezawa A.</u>	Human dystrophin expression in the mdx mouse, a model of Duchenne muscular dystrophy, can be conferred predominantly by "cell fusion" with human menstrual blood-derived cells.	Mol Biol Cell.	18(5)	1586-94	2007
<u>Umezawa A.</u> Toyoda M.	Two MSCs : Marrow stromal cells and mesenchymal stemcells.	Inflammation and Regeneration.	27(1)	28-36	2007
Yamada Y, Sakurada K, Takeda Y, Gojo S, <u>Umezawa A.</u>	Single-cell-derived mesenchymal stem cells overexpressing Csx/Nkx2.5 and GATA4 undergo the stochastic cardiomyogenic fate and behave like transient amplifying cells.	Exp Cell Res.	313	698-706	2007
Sugiki T, Uyama T, Toyoda M, Morioka H, Kume S, Miyado K, Matsumoto K, Saito H, Tsumaki N, Takahashi Y, Toyama Y, <u>Umezawa A.</u>	Hyaline cartilage formation and enchondral ossification modeled with KUM5 and OP9 chondroblasts.	J Cell Biochem.	100(5)	1240-54	2007
Yokoi T.,Saito M., <u>Kiyono T.</u> ,Iseki S.,Kosaka K.,Nishida E.,Tsubakimoto T.,Harada H.,Eto K.,Noguchi T.,Teranaka T.	Establishment of immortalized dental follicle cells for generating periodontal ligament in vivo	Cell Tissue Res	327	301-11	2007
<u>Kiyono T.</u>	Molecular mechanisms of cellular senescence and immortalization of human cells.	Expert Opin Biol Ther.	11	1623-37	2007
Shiga M.,Saito M.,Hattori M.,Torii C.,Kosaki K., <u>Kiyono T.</u> ,Suda N.	Characteristic phenotype of immortalized periodontal cells isolated from a Marfan syndrome type I patient.	Cell Tissue Res.	331	461-472	2008
Into T, Inomata M, Nakashima M, Shibata K, Häcker H, <u>Matsushita K.</u>	Regulation of MyD88-dependent signaling events by S nitrosylation retards toll-like receptor signal transduction and initiation of acute-phase immune responses.	Mol Cell Biol.	28(4)	1338-1347	2008
Kanno Y, Into T, Lowenstein CJ, <u>Matsushita K.</u>	Nitric oxide regulates vascular calcification by interfering with TGF- signalling.	Cardiovas c Res.	77(1)	221-230	2008
Inomata M., Into T., Ishihara Y., Nakashima M., Noguchi T., and <u>Matsushita K.</u>	Arginine-specific gingipain A from Porphyromonas gingivalis induces Weibel-Palade body exocytosis and enhanced activation of vascular endothelial cells through protease-activated receptors.	Microbes Infect.	9 (12-13)	1500-1506	2007
Into, T., Dohkan, J., Inomata, M., Nakashima, M., Shibata, K., and	Synthesis and characterization of a dipalmitoylated lipopeptide derived from	Infect	75(5)	2253-2259	2007

<u>Matsushita, K.</u>	paralogous lipoproteins of Mycoplasma pneumoniae.	Immun.			
Into, T., Kanno, Y., Dohkan, J., Nakashima, M., Inomata, M., Shibata, K., Lowenstein, C.J., and <u>Matsushita, K.</u>	Pathogen recognition by Toll-like receptor 2 activates Weibel-Palade body exocytosis in human aortic endothelial cells.	J. Biol. Chem.	282(11)	8134-8141	2007
Zheng L, Iohara K, Ishikawa M, Into T, Takano-Yamamoto T, <u>Matsushita K</u> , Nakashima M.	Runx3 negatively regulates Osterix expression in dental pulp cells.	Biochem J.	405(1)	69-75	2007
齋藤正寛	歯科再生医療はどこまで到達し、どこへ向かうのか？歯根再生のキーワードとして[HERS]のメカニズムに迫る-ESTデータベースを用いた歯根膜発生機構の解析-	歯界展望	impres s		
齋藤正寛、辻 孝	臓器置換技術を応用した次世代歯科再生医療の開発	デンタルダイヤモンド	第32巻	80-84	2007
村上伸也、島袋善夫、北村正博、山田 聡	歯周組織再生医療とDDS技術に期待するもの	日本再生医療学会雑誌	第6巻	32-41	2007
村上伸也、橋川智子	歯周組織再生の現状と将来の展望 再生医学のいま —基礎研究から臨床への展開に向けて-	治療	第90巻	609-616	2008

#### IV. 研究成果の刊行物・別冊

# Neurotrophic Factor Neurotrophin-4 Regulates Ameloblastin Expression via Full-length *TrkB*<sup>\*[5]</sup>

Received for publication, June 14, 2007, and in revised form, October 31, 2007. Published, JBC Papers in Press, November 28, 2007, DOI 10.1074/jbc.M704913200

Keigo Yoshizaki<sup>†‡§</sup>, Shinya Yamamoto<sup>‡</sup>, Aya Yamada<sup>‡</sup>, Kenji Yuasa<sup>‡</sup>, Tsutomu Iwamoto<sup>‡</sup>, Emiko Fukumoto<sup>¶</sup>, Hidemitsu Harada<sup>||</sup>, Masahiro Saito<sup>\*\*</sup>, Akihiko Nakasima<sup>§</sup>, Kazuaki Nonaka<sup>‡</sup>, Yoshihiko Yamada<sup>††</sup>, and Satoshi Fukumoto<sup>‡§§1</sup>

From the Section of <sup>‡</sup>Pediatric Dentistry and <sup>§</sup>Orthodontics, Division of Oral Health, Growth, and Development, Faculty of Dental Science, Kyushu University, Fukuoka 812-8582, Japan, <sup>¶</sup>Nagasaki University Graduate School of Biomedical Sciences, Nagasaki 852-8521, Japan, the <sup>||</sup>Department of Oral Anatomy II, Iwate Medical College School of Dentistry, Morioka, Iwate 020-8505, Japan, the <sup>\*\*</sup>Department of Molecular and Cellular Biochemistry, Osaka University Graduate School of Dentistry, Suita, Osaka 565-0871, Japan, the <sup>††</sup>Craniofacial Developmental Biology and Regeneration Branch, NIDCR, National Institutes of Health, Bethesda, Maryland 20892, and the <sup>§§</sup>Division of Pediatric Dentistry, Department of Oral Health and Development Sciences, Tohoku University Graduate School of Dentistry, Sendai, Miyagi 980-8575, Japan

Neurotrophic factors play an important role in the development and maintenance of not only neural but also nonneural tissues. Several neurotrophic factors are expressed in dental tissues, but their role in tooth development is not clear. Here, we report that neurotrophic factor neurotrophin (NT)-4 promotes differentiation of dental epithelial cells and enhances the expression of enamel matrix genes. Dental epithelial cells from 3-day-old mice expressed NT-4 and three variants of *TrkB* receptors for neurotrophins (full-length *TrkB-FL* and truncated *TrkB-T1* and *-T2*). Dental epithelial cell line HAT-7 expressed these genes, similar to those in dental epithelial cells. We found that NT-4 reduced HAT-7 cell proliferation and induced the expression of enamel matrix genes, such as ameloblastin (*Ambn*). Transfection of HAT-7 cells with the *TrkB-FL* expression construct enhanced the NT-4-mediated induction of *Ambn* expression. This enhancement was blocked by K252a, an inhibitor for *Trk* tyrosine kinases. Phosphorylation of ERK1/2, a downstream molecule of *TrkB*, was induced in HAT-7 cells upon NT-4 treatment. *TrkB-FL* but not *TrkB-T1* transfection increased the phosphorylation level of ERK1/2 in NT-4-treated HAT-7 cells. These results suggest that NT-4 induced *Ambn* expression via the *TrkB*-MAPK pathway. The p75 inhibitor TAT-pep5 decreased NT-4-mediated induction of the expression of *Ambn*, *TrkB-FL*, and *TrkB-T1*, suggesting that both high affinity and low affinity neurotrophin receptors were required for NT-4 activity. We found that NT-4-null mice developed a thin enamel layer and had a decrease in *Ambn* expression. Our results suggest that NT-4 regulates proliferation and differentiation of the dental epithelium and promotes production of the enamel matrix.

Mammalian development is a complex and highly orchestrated process that involves intricate cross-talk between growth factors and other regulatory molecules. The interaction between the epithelium and mesenchyme induces specific molecular and cellular changes that lead to organogenesis. These interactions are particularly crucial during the initiation of the development of ectodermal organs, such as teeth, skin, hair, and mammary and prostate glands (1). The oral epithelium provides the initial signaling for neuronal crest-derived ectomesenchyme development, and then both tissues interact during tooth formation. Various transcription factors, growth factors, and extracellular matrices are expressed by enamel matrix-producing ameloblasts during tooth development (2–4). The principal components of the enamel matrix that are synthesized by secretory ameloblasts can be classified into two major categories, amelogenin (*Amel*)<sup>2</sup> and non-*Amel*, which includes ameloblastin (*Ambn*) and enamelin (*Enam*) (5). *Ambn*, also known as amelin or sheathlin, is a tooth-specific glycoprotein that represents the most abundant non-*Amel* enamel matrix protein. We previously created *Ambn*-null mice, which develop severe enamel hypoplasia in which ameloblasts detached from the matrix, lost cell polarity, resumed proliferation, and formed multiple cell layers (6). These results suggest that *Ambn* is essential for ameloblast differentiation and enamel formation.

Nerve growth factor (NGF), brain-derived neurotrophic factor (BDNF), and neurotrophin-3 and -4/5 (NT-3 and NT-4/5, respectively) are structurally and functionally related and belong to the neurotrophin family, which promotes the development and survival of the vertebrate nervous system (7). Neurotrophins interact with two classes of cell surface receptors. The first class is *Trk* tyrosine kinase receptors that bind neurotrophins with a high affinity (8). *TrkA* mediates the biological

\* This work was supported in part by Grants-in-aid for Research Fellows 15689025, 17689058, 19791585, and 17659650 from the Japan Society for the Promotion of Science and the Ministry of Education, Science, and Culture of Japan (to S.F., A.Y., and K.N.). The costs of publication of this article were defrayed in part by the payment of page charges. This article must therefore be hereby marked "advertisement" in accordance with 18 U.S.C. Section 1734 solely to indicate this fact.

[5] The on-line version of this article (available at <http://www.jbc.org>) contains supplemental Table 1 and Figs. 1–3.

<sup>1</sup> To whom correspondence should be addressed: Division of Pediatric Dentistry, Dept. of Oral Health and Development Sciences, Tohoku University Graduate School of Dentistry, Sendai, Miyagi 980-8575, Japan. Fax: 81-22-717-8380; E-mail: fukumoto@mail.tains.tohoku.ac.jp.

<sup>2</sup> The abbreviations used are: *Amel*, amelogenin; BrdUrd, bromo-2'-deoxyuridine; MAPK, mitogen-activated protein kinase; ERK, extracellular signal-regulated kinase; *Ambn*, ameloblastin; *Enam*, enamelin; NGF, neural growth factor; BDNF, brain-derived neurotrophic factor; NT, neurotrophin; PBS, phosphate-buffered saline; RT, reverse transcriptase; MEK, mitogen-activated protein kinase/extracellular signal-regulated kinase kinase; P1, P3, and P7, postnatal day 1, 3, and 7, respectively.

## NT-4 Regulates Ameloblastin Expression

response of NGF, *TrkC* is activated by NT-3, and BDNF and NT-4/5 are the preferred ligands for *TrkB* (7). *TrkB* and *TrkC* have truncated transcripts at the C terminus (9–12). The second class is the common low affinity neurotrophin receptor, p75, which does not have a tyrosine kinase domain (13, 14). Further, neurotrophins have other regulatory roles during embryogenesis. NGF is a mitogenic factor for human epithelial cells (15), and NT-3 stimulates the proliferation of migratory neural crest cells (16). The expression of p75 may be required for kidney morphogenesis (17) and also promote apoptosis (18, 19). In the skin, the expression of BDNF and NT-4 is strikingly dependent on the hair cycle and peaks during spontaneous, apoptosis-driven hair follicle regression, known as catagen. NT-4 was also reported to accelerate catagen development in murine skin organ cultures. These results suggest that NT-4 is useful as an agent of hair growth control.

During tooth development, neurotrophic factors and their receptors are expressed in the tooth germ (20). However, their role in tooth development has not been elucidated. At the initiation stages of tooth germ development, NGF is expressed in the dental mesenchyme and weakly in the dental epithelium. At the bud stage, the majority of dental epithelial cells have lost their NGF expression, although NGF is still expressed in the inner dental epithelium and condensed mesenchyme. During later embryonic and early postnatal tooth development, NGF can be observed in the dental follicles. At the bell stage, NGF appears in epithelial cells of the stratum intermedium, whereas after birth it is restricted to cells located in the cervical part of the enamel organ. In the postnatal period, NGF is also detected in the dental papilla mesenchyme. BDNF is expressed in the region of developing rat teeth as well as in the mesenchyme under the developing skin of the mandibular process (20). In postnatal animals, BDNF is mainly detected in the dental papilla, and its expression pattern is correlated with the onset of dental innervation (21). NT-3 is expressed throughout the mesenchyme of the mandibular process at the initiation stage, whereas it appears in the epithelial cervical loops in the cap stage. During later stages, NT-3 expression is gradually restricted to the more cervical parts of the inner enamel epithelium and is no longer detected in postnatal tooth germs (20). The expression of NT-4 is restricted to epithelial cells. During subsequent development, expression persists in all dental epithelium components, including ameloblasts and the outer enamel epithelium as well as in the dental lamina (20, 21). Among neurotrophic factors, NT-4 is the only one detected in differentiated ameloblasts. These findings suggest that NT-4 may be important for dental epithelium differentiation and maintenance of ameloblast functions. However, the role of NT-4 in tooth development is unknown.

In the present study, we investigated the roles of NT-4 and *TrkB* in tooth development *in vitro* using dental epithelium cultures and *in vivo* using NT-4 knock-out mice. NT-4 and *TrkB* receptors were expressed in the dental epithelium of 3-day-old mice and in the HAT-7 dental epithelial cell line. We found that NT-4 inhibited proliferation and induced differentiation of HAT-7 cells. NT-4 treatment of HAT-7 cells increased mRNA expression for enamel matrix proteins *Ambn*, *Enam*, and dentin sialophosphoprotein. Further, NT-4-mediated

induction of *Ambn* expression was regulated by the full-length *TrkB-FL* receptor and ERK1/2 pathway. In NT-4 knock-out mice, *Ambn* expression was dramatically reduced, and the enamel layer was thin. Our findings suggest that NT-4 plays a role in proliferation and differentiation of the dental epithelium and is required for the expression of enamel matrix genes.

### EXPERIMENTAL PROCEDURES

**Cell Culture and Transfection**—HAT-7 cells, an epithelial cell line, and mDP cells, a dental mesenchymal cell line, were maintained in Dulbecco's modified Eagle's medium/F-12 medium supplemented with 10% fetal bovine serum and 1% penicillin and streptomycin at 37 °C in a humidified atmosphere containing 5% CO<sub>2</sub> (22). To transfect with the expression vectors for *TrkB*, HAT-7 cells were plated in a 60-mm plastic tissue culture plate (Falcon) at a density of 1 × 10<sup>6</sup> cells/3 ml/plate. To facilitate the detection of protein expression, V5 and His tags were fused to the C terminus of the two rat *TrkB* isoforms, *TrkB-FL* and *TrkB-T1*. *TrkB-FL* and *TrkB-T1* cDNA were prepared from adult rat brain mRNA by RT-PCR and confirmed by DNA sequencing. The forward primer for *TrkB-FL* and *TrkB-T1* was 5'-CTCTGACTGACTGGACTGG-3', and the reverse primer was 5'-GCCTAGGATGTCCAGGTAGACGGGC-3' for *TrkB-FL* or 5'-CCCATC-CAGGGGATCTTA-3' for *TrkB-T1*. PCR was performed at 94 °C for 30 s, 60 °C for 30 s, and 72 °C for 60 s for 30 cycles. The PCR products were cloned into pEF6/V5-His-TOPO® (Invitrogen) according to the manufacturer's protocol. Cells were transfected using Lipofectamine 2000 (Invitrogen) according to the manufacturer's protocol. Stable transfectant cells for *TrkB-FL* and *TrkB-T1* were selected in the presence of 5 μg/ml Blasticidin (Invitrogen).

**Cell Proliferation and Bromodeoxyuridine (BrdUrd) Incorporation**—Cells were plated at 1 × 10<sup>5</sup> cells/ml/well in 12-well plates for 24 h. Cell numbers were determined using a trypan blue dye exclusion method. For the BrdUrd incorporation assay, cells were incubated at the same cell density described above for 24 h prior to the addition of various growth factors. After treatments with various growth factors, BrdUrd (Sigma) was added to the plates (10 μM) for 30 min, and then the cells were fixed with cold methanol for 10 min, rehydrated in phosphate-buffered saline (PBS), and incubated for 30 min in 1.5 M HCl. After washing three times in PBS, the plates were incubated with a 1:50 dilution of fluorescein isothiocyanate-conjugated anti-BrdUrd antibody (Roche Applied Science) for 30 min at room temperature. Finally, the cells were washed in PBS three times and incubated with 10 μg/ml propidium iodide (Sigma) in PBS for 30 min at room temperature. BrdUrd-positive cells were examined under a microscope (Biozero-8000; Keyence, Japan).

**Western Blotting**—Cells were plated in 12-well plates at 1 × 10<sup>5</sup> cells/well for 1 day prior to NT-4 treatment. The cells were then treated with 100 ng/ml NT-4 for 0–60 min at 37 °C. Thereafter, they were washed twice with ice-cold 1 mM sodium orthovanadate (Sigma) in PBS, lysed with Nonidet P-40 buffer supplemented with a proteinase inhibitor mixture (Sigma) and phenylmethanesulfonyl fluoride at 4 °C for 10 min, and centrifuged, and then the supernatants were transferred to a fresh



tube. The cell lysates were separated by 12% SDS-PAGE and analyzed by Western blotting. The blotted membrane was incubated with antibodies, and the signals were detected with an ECL kit (Amersham Biosciences). ERK and second antibodies were purchased from Cell Signaling.

**RNA Isolation and RT-PCR**—Developing molars were dissected from mice on postnatal day 1 (P1), P3, and P7. Epithelial and mesenchymal tissues were separated from tooth germ from P3 mice under a microscope. Total RNA was isolated using TRIzol (Invitrogen) according to the manufacturer's protocol. First strand cDNA was synthesized at 42 °C for 90 min using oligo(dT)<sub>14</sub> primer with SuperScript III (Invitrogen). PCR amplification was performed using the primers listed in supplemental Table 1. The PCR products were separated on a 1.5% agarose gel. The relative expression level was deduced from a standard curve constructed using the positive control sample and normalized against the expression level of HPRT in each sample.

**Protein Kinase-inhibitory Assay**—Serum-deprived HAT-7 cells were plated in 6-well plates and treated with 0.5 μM K-252a (*Trk* tyrosine kinase inhibitor; Calbiochem) and 100 nM TAT-Pep5 (p75NTR signaling inhibitor; Calbiochem) prior to treatment with NT-4 for 30 min. After 48 h, total RNA was extracted, and RT-PCR was performed.

**Preparation of Tissue Sections and HE Staining**—Mouse heads from P1, P3, and P7 wild-type and NT-4 null mice were fixed with 4% paraformaldehyde in PBS overnight at 4 °C. The tissues were decalcified with 250 mM EDTA/PBS for 3 days, dehydrated in xylene through a graded ethanol series, and then embedded in paraffin. Sections were sliced at 8 μm using a microtome (RM2125RT; Leica). For detailed morphological analysis of the molars, the sections were stained with Harris hematoxylin (Sigma) and Eosine Y (Sigma). The widths of enamel matrix and dentin were measured under a microscope (Bisozero-8000).

## RESULTS

**Expression of NT-4 and *TrkB* Receptors in the Tooth Germs and Dental Cell Lines**—We first examined the expression of NT-4 and *TrkB* receptors in tooth germs and dental cell lines by RT-PCR. In tooth germs of P3 mice, NT-4 was highly expressed in the dental epithelium and weakly expressed in the dental mesenchyme (Fig. 1A). The full-length *TrkB-FL* and truncated *TrkB-T1* and *-T2* were expressed in the dental epithelium. On the other hand, *TrkB-T1*, but not *TrkB-FL* or *TrkB-T2*, was expressed in the mesenchyme. Further, p75 expression levels were low in both the epithelium and mesenchyme (Fig. 1A). The expression patterns of NT-4, *TrkB*s, and p75 in dental epithelial cell line HAT-7 and dental mesenchyme cell line mDP were similar to those in the tooth germ tissues, except for a low expression level of *TrkB-FL* in mDP cells and a high expression level of p75 in HAT-7 cells (Fig. 1B). These results suggest that NT-4, *TrkB-FL*, *TrkB-T1*, and *TrkB-T2* are expressed in the dental epithelium and may regulate differentiation of the dental epithelium.

**Inhibition of Proliferation of HAT-7 Cells by NT-4**—We next examined the effect of NT-4 on HAT-7 cell proliferation (Fig. 2). HAT-7 cells were treated with NT-4, and cell proliferation was analyzed by BrdUrd incorporation for 1 h. The number of

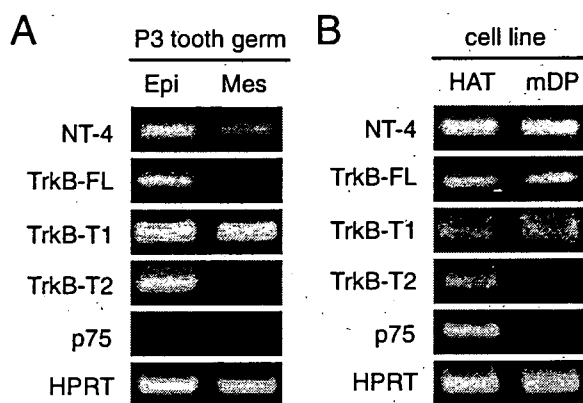


**FIGURE 1. Expression of NT-4 and receptors in tooth germs and dental cell lines.** Tooth germs were dissected from P3 mice, and the dental epithelium (*Epi*) and mesenchyme (*Mes*) were separated under a microscope. Total mRNA from these tissues was amplified using a semiquantitative RT-PCR method with specific primer sets (A). Total mRNA expression of NT-4 and *TrkB* receptors in dental epithelial cell line HAT-7 and mesenchymal cell line mDP was analyzed by RT-PCR (B).

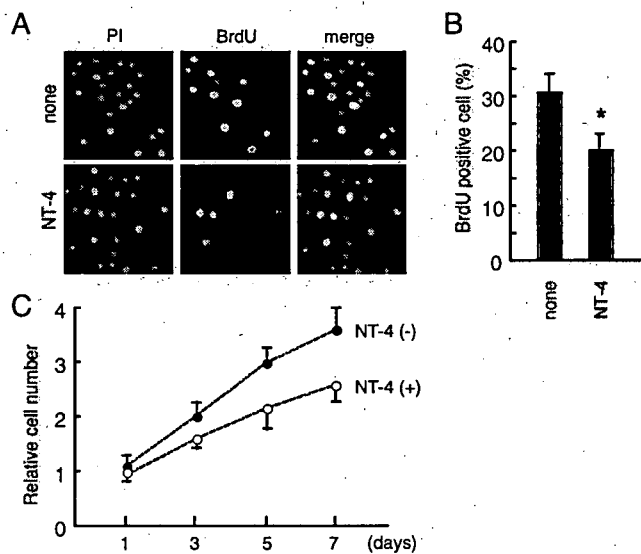


**FIGURE 2. NT-4 inhibits cell proliferation.** Dental epithelial cells (HAT-7) were cultured with NT-4 for 24 h. BrdUrd incorporation after 1 h was analyzed using a fluorescence microscope (A and B). Cell numbers of HAT-7 cells cultured with or without NT-4 were counted using a trypan blue exclusion method after 1, 3, 5, and 7 days of culture (C). These experiments were repeated at least five times with similar results. Statistical analysis was performed using analysis of variance (\*,  $p < 0.01$ ).

BrdUrd-positive cells was decreased by 30% after stimulation with NT-4 (Fig. 2, A and B). We also found that the number of HAT-7 cells was decreased by about 25% when the cells were cultured in the presence of NT-4 for 7 days (Fig. 2C). These results indicate that NT-4 inhibits the proliferation of dental epithelial cells in culture.

**NT-4 Induces *Ambn* Expression**—To analyze the effects of neurotrophic factors on dental epithelium differentiation, NGF, BDNF, or NT-4 was added to HAT-7 cell cultures. After 48 h, total RNA was analyzed for the expression of ameloblast differentiation markers by RT-PCR. *Ambn*, *Enam*, dentin sialophosphoprotein (*Dspp*), osteopontin (*Opn*), and osteonectin (*Osn*) were induced by NGF, BDNF, and NT-4 (Fig. 3, A and B).

## NT-4 Regulates Ameloblastin Expression

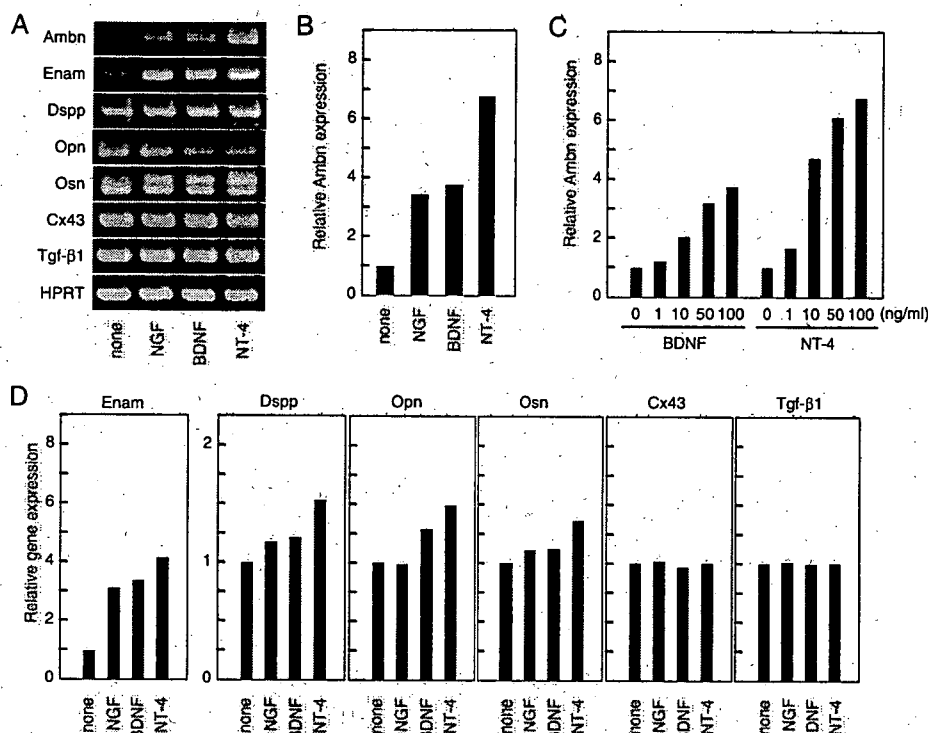


**FIGURE 3. Expression of tooth marker genes in HAT-7 cells with neurotrophic factors.** HAT-7 cells were cultured with 100 ng/ml NGF, BDNF, or NT-4 for 48 h. Total mRNA was analyzed for the expression of various genes by semiquantitative RT-PCR. Ambn, Enam, dentin sialophosphoprotein (*Dspp*), osteopontin (*Opn*), osteonectin (*Osn*), connexin 43 (*Cx43*), and transforming growth factor- $\beta$ 1 (*Tgf- $\beta$ 1*) (A). Hprt was used as an internal control. The level of gene expression in the absence of growth factors was set at 1 for comparison (B and D). HAT-7 cells were stimulated with various amounts of NT-4 and BDNF for 48 h. Hprt expression showed no significant difference between each culture. The level of Ambn expression in cells without factors was set at 1 for comparison (C).

Amel was also induced by NT-4 (data not shown). This effect was similar on all of the various amelogenin isoforms. The expression level of Ambn induced by NT-4 was higher than those by NGF or BDNF (Fig. 3B). The induction of Ambn expression by BDNF or NT-4 was dose-dependent (Fig. 3C), with the higher level by NT-4. The expression of gap junctional proteins (*Gja1*) and transforming growth factor- $\beta$ 1 was the same between the control and neurotrophic factor-treated cells (Fig. 3D). These results indicate that NT-4 induces enamel matrix genes and promotes ameloblast differentiation.

**NT-4 and BDNF Induce Expression of Their Receptor but Not p75**—Since the expression level of *TrkB* receptors is important for NT-4 signaling, we examined their expression in HAT-7 cells with or without NT-4 by RT-PCR (supplemental Fig. 1). We found that *TrkB-FL*, *TrkB-T1*, and *TrkB-T2* were highly induced by NT-4 and BDNF. NGF also induced the expression of *TrkB-FL* and *TrkB-T1*, but not *TrkB-T2* (supplemental Fig. 1, A and B).

**Overexpression of *TrkB-FL* Enhances NT-4-mediated Ambn Induction**—NT-4 induced expression of Ambn, *TrkB-FL*, and truncated *TrkB*. However, it is not clear which receptor is active for NT-4-mediated Ambn induction. To assess this question, we stably transfected HAT-7 cells with the *TrkB-FL* or *TrkB-T1* expression construct, cultured them with NT-4, and analyzed Ambn expression by RT-PCR. Ambn expression was induced by NT-4 in untransfected cells as shown in Figs. 3, A and B, and

4A. This NT-4-mediated Ambn induction was increased in *TrkB-FL*-transfected cells (Fig. 4, A and B). The basal level of Ambn expression was also higher in the transfected cells than in untransfected cells. However, in *TrkB-T1*-transfected cells, NT-4-mediated Ambn induction was inhibited (Fig. 4, A and B). Similar results were obtained from immunohistological analysis using Ambn antibody (data not shown). Furthermore, Ambn expression induced by NT-4 in *TrkB-FL* transfectants was completely inhibited by K252a, a *Trk* tyrosine kinase inhibitor (Fig. 4, C and D). These results indicate that the induction of Ambn by NT-4 is regulated via *TrkB-FL* but not by truncated *TrkB-T1*.

**NT-4 Activates ERK1/2**—In neuronal cells, NT-4 induces phosphorylation of *TrkB* and activates the Ras-MEK-ERK1/2 pathway (8). To analyze NT-4 signaling in the dental epithelium, we performed Western blotting using anti-phospho-specific ERK1/2 (MAPK) antibody. Phosphorylation of ERK1/2 was observed at 5 min after stimulation with NT-4 and then disappeared after 30 min (Fig. 5A). Further, the level of phosphorylation of ERK2 was higher than that of ERK1 (Fig. 5B). Next, we examined the ERK1/2 phosphorylation level in *TrkB*-transfected HAT-7 cells in the presence of NT-4 (Fig. 6, A and B). *TrkB-FL*-transfected cells showed strong activation of ERK1/2 at 5 min after the NT-4 treatment. However, the activation of ERK1/2 was not observed in *TrkB-T1*-transfected cells. These results indicate that full-length *TrkB-FL* is a major *TrkB* receptor for NT-4 signaling, and truncated *TrkB-T1* acts as a dominant negative factor for dental epithelial cells.

***Trk* Inhibitor K252a Inhibits Ambn Expression**—NT-4 binds to *TrkB* and the low affinity receptor p75 and transduces downstream cellular signaling (8). To identify the signaling pathway involved in Ambn expression, we treated HAT-7 cells with the *Trk* inhibitor K252a or p75 inhibitor TAT-pep5 prior to stimulation with NT-4 (Fig. 7, A and B). NT-4-mediated induction of Ambn was significantly inhibited by K252a and TAT-pep5. Moreover, the induction of *TrkB* receptors by NT-4 was also inhibited by K252a and TAT-pep5. The inhibitory effect by K252a was higher than that by TAT-pep5. The MEK inhibitor PD98059 inhibited phosphorylation of neurotrophic factor-induced ERK1/2, and PD98059 treatment also inhibited the NT-4-mediated Ambn induction in HAT-7 cells (data not shown). These results suggest that ligand-induced activation of *TrkB* and p75 is important for the expression of Ambn, *TrkB-FL*, and *TrkB-T1*.

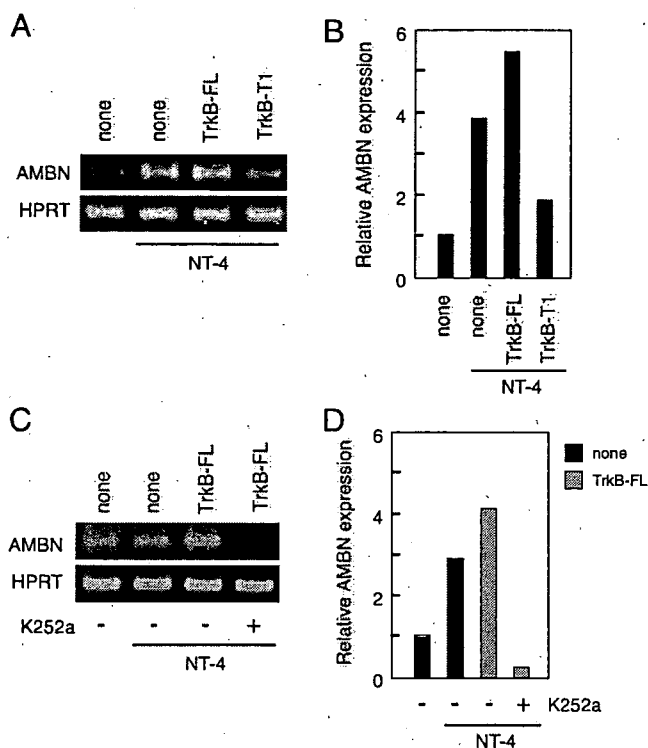


**FIGURE 4. Increase in NT-4-mediated Ambn induction in HAT-7 cells by overexpressing TrkB-FL.** The expression constructs for *TrkB-FL* and *TrkB-T1* receptors were stably transfected into HAT-7 cells. The pooled transfected cells were treated with NT-4 for 48 h. Ambn expression was analyzed using RT-PCR (A). The level of Ambn expression in the control cells without NT-4 was set at 1 for comparison (B). The *TrkB-FL* transfectant cells were cultured with or without K252a in the presence of NT-4 for 48 h and then analyzed for the expression of Ambn (C). The level of gene expression in the control cells without NT-4 was set at 1 for comparison (D).

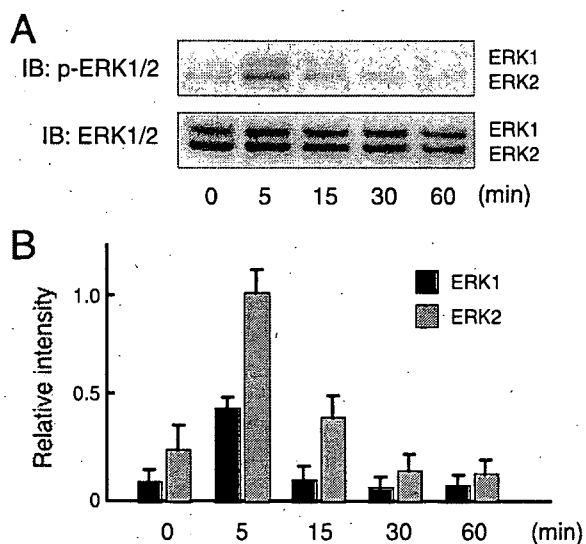


**FIGURE 5. Phosphorylation of ERK1/2 stimulated by NT-4.** The time course of phosphorylation of ERK1/2 after NT-4 treatment was analyzed by Western blotting (IB) using the anti-phospho-MAPK antibody (A). For the quantitations of A, the relative intensity of phosphorylated ERK1/2 (p-ERK1/2) in HAT-7 cells after 5 min was set at 1 for comparison (B).

**NT-4 Null Mice Develop a Thin Enamel Layer and Have Reduced Ambn Expression**—We demonstrated that NT-4 promoted epithelia cell differentiation in culture. To examine *in vivo* function of NT-4 in tooth development, we analyzed molars of NT-4 null mice (Fig. 8). NT-4 expression was completely absent in tooth germs of P1, P3, and P7 mice (supplemental Fig. 3). The expression of *TrkB* in NT-4 null tooth germs was similar to that of heterozygotes and wild-type mice (data not shown). We found that P3 molars had a thinner enamel matrix layer than control, whereas there was no significant difference in the predentin and dentin (Fig. 8, A and B). The size, shape, and polarization of ameloblasts in the mutant molars were normal as compared with those of the heterozygotes. Furthermore, Ambn expression in NT-4 null tooth germs was reduced as compared with that in heterozygotes (Fig. 8, C and D). These results suggest that NT-4 regulates Ambn expression and enamel layer formation.

**DISCUSSION**

Our results show that NT-4 regulates dental epithelial cell differentiation and enamel matrix gene expression via *TrkB-FL* but not via truncated *TrkB* forms. NT-4 inhibited cell proliferation and also induced enamel matrix genes, such as Ambn in dental epithelial cells. NT-4-deficient teeth resulted in a thin enamel layer during the initial stage of amelogenesis. Our findings are the first to show that a neurotrophic factor plays an important role in tooth development.

The functional roles of NT-4 and its receptors have been reported mainly in neuronal tissues. Complete ablation of p75 in mice causes defects in both the nervous and vascular systems (23). Those animals displayed sensory and sympathetic defects, thus demonstrating that the p75 receptor is required for proper neuronal development. *TrkB* mutants display severe phenotypes that result in the death of most mutant mice in the first postnatal week because of their inability to feed (24), whereas NT-4 knock-out mice are viable and fertile but have a 50% loss of neurons in the nodose-petrosal and geniculate ganglia (25, 26). BDNF knock-out mice are characterized by selective sensory disorders and have a reduced number of neurons in sensory ganglia; they do not survive longer than 3–4 weeks after birth (27, 28). Although NT-4 and BDNF use *TrkB* as a receptor, phenotypes of *TrkB*, NT-4, and BDNF knock-out mice differ each other. Thus, it is suggested that NT-4 has a different expression pattern and function from that of BDNF. In fact, NT-4, but not BDNF, is expressed in the inner dental epithelium. During tooth germ development, NGF is expressed in the dental mesenchyme but not in the dental epithelium (20). In contrast, BDNF is found in the dental mesenchyme in the human tooth germ but not in that of mice. In the present study, both NGF and BDNF induced expression of the ameloblast markers, Ambn and Enam, and NT-4 receptors, *TrkB-FL* and *TrkB-T1*. NGF and BDNF may be important for mesenchymal and epithelial interactions. NT-4 was expressed mostly in dental epithelia in tooth germs and has been detected in both dental epithelial and mesenchymal cell lines, suggesting that it functions in an autocrine manner in dental epithelium. We found that p75 was expressed in an undifferentiated dental epithelial cell line but was not detectable in the tooth germ. It was

Downloaded from www.jbc.org at OSAKA UNIVERSITY on March 5, 2008

## NT-4 Regulates Ameloblastin Expression

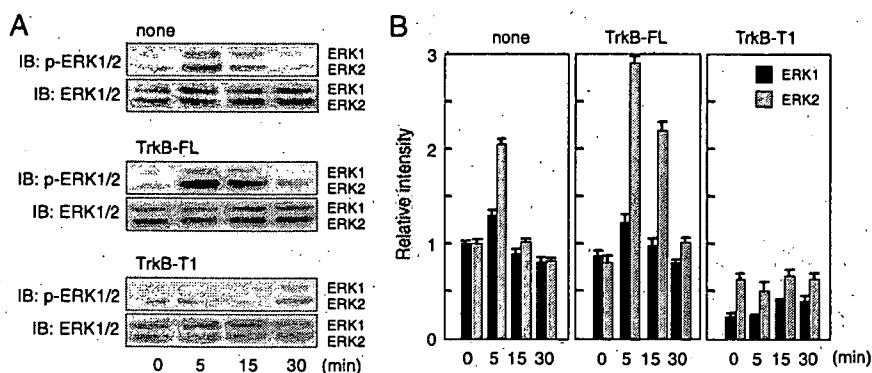


**FIGURE 6. Increase in phosphorylation of ERK1/2 in *TrkB-FL* transfectant cells by NT-4.** The time course of phosphorylation of ERK1/2 in *TrkB-FL* and *T1*-transfected HAT-7 cells after treatment with NT-4 was analyzed by Western blotting (IB) using the anti-phospho-MAPK antibody (A). The Western blots with anti-MAPK showed equivalent amounts of total ERK proteins in each lane. The relative intensity of p-ERK1 in the control cells at 0 min was set at 1 for comparison (B).

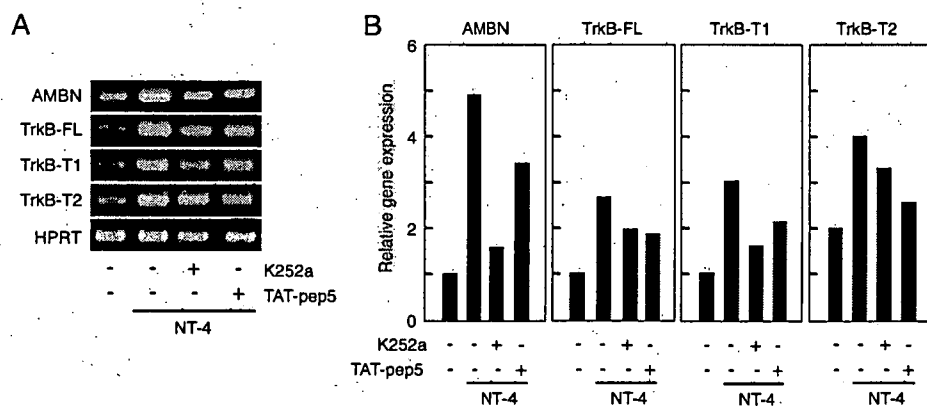


**FIGURE 7. Inhibition of NT-4-mediated induction of *Ambn* and *TrkBs* by K252a and TAT-pep5.** HAT-7 cells were treated with NT-4 in the presence of K252a or TAT-pep5. The expressions of *Ambn*, *TrkB-FL*, *TrkB-T1*, and *TrkB-T2* were analyzed by semiquantitative RT-PCR with specific primer sets (A). The level of gene expression in the control cells without NT-4 was set at 1 for comparison (B).

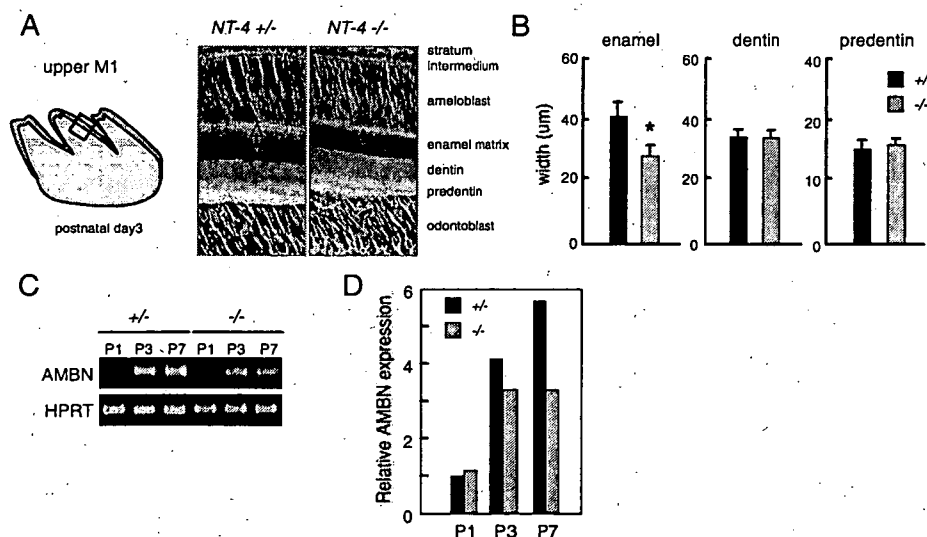


**FIGURE 8. Decrease in the enamel matrix width and expression of *Ambn* in NT-4 null mice.** Hematoxylin and eosin staining of P3 mouse molars were performed (A). The widths of the enamel matrix, dentin, and predentin were measured (B). Developing molars from heterozygote and mutant mice were dissected from P1, P3, and P7 mice, and total mRNA was prepared. The expression of *Ambn* was analyzed by semiquantitative RT-PCR with an *Ambn* primer set (C). The level of *Ambn* expression in P1 heterozygote mice was set at 1 for comparison (D).

reported that in incisors, p75 is expressed in the inner dental epithelium but is completely absent in differentiated ameloblasts (6). Further, the possibility of epithelial-mesenchymal communication within the intact tooth germ, whereas there is complete absence of those effects in the individual cells cultures, may be at the root of the differences of p75 expression between tooth germ and dental epithelial cell cultures. Moreover, p75 expression was not changed after stimulation with neurotrophins, whereas the p75 inhibitor TAT-pep5 was less effective on the expression of *Ambn* than *Trk* inhibitor K252a. These results suggest that p75 may not be important for the expression of *Ambn* in ameloblasts.

Truncated *TrkB* receptors have dominant inhibitory effects on BDNF and presynaptic signaling for BDNF-induced synaptic potentiation in cultured hippocampal neurons (29, 30). Truncated *TrkB-T1* mediates neurotrophin-evoked calcium signaling in glia cells (31) and plays a direct signaling role in mediating inositol-1,4,5-trisphosphate-dependent calcium release. In developing teeth, *TrkB-T1*, but not *TrkB-FL* or *TrkB-T2*, is detected by *in situ* hybridization (32). In the present study, all types of *TrkB* were detected in P3 tooth germ epithelia and a dental epithelial cell line. This discrepancy of *TrkB* expression may have occurred because of different detection efficiencies of the methods used. Although both *TrkB-FL* and truncated *TrkB* were induced by NT-4, overexpression of *TrkB-FL* enhanced the expression of *Ambn*, but *TrkB-T1* had a dominant negative effect on NT-4-induced *Ambn* expression. In NT-4-null mice, the expression of *TrkB-T1* and *-T2* was not changed from normal levels. These results suggest that truncated *TrkB* does not have an inhibitory effect on *Ambn* expression induced by NT-4.

*Ambn* plays an important role in maintaining the differentiation state of ameloblasts, serves as a cell

adhesion molecule, and inhibits the proliferation of the dental epithelium (6). A deficiency of *Ambn* causes severe enamel hypoplasia, accelerates proliferation of the dental epithelium, and decreases the expression of amelogenin. The *Ambn* promoter functions in a cell type-specific manner and contains cis-acting elements that function to enhance and suppress transcription (33). The transcription factor *Runx2*, known as an essential factor for transcription of mineralized tissue genes, is also required for *Ambn* transcription (33). Site-directed mutagenesis of the *Runx2*-binding site in the *Ambn* promoter decreases *Ambn* promoter activity in the dental epithelium (33). Sp3, a member of the Sp family of transcription factors, is ubiquitously expressed and present in ameloblasts at the pre-secretory and secretory stages but not the maturation stage. Sp3-deficient embryos show growth retardation and invariably die at birth of respiratory failure (34), and both endochondral and intramembranous ossification are impaired (35). These mice also have a pronounced defect in late tooth formation. In Sp3-null mice, the enamel and dentin layers of teeth are impaired due to the lack of ameloblast-specific gene products, including *Ambn*. These results indicate that *Runx2* and Sp3 are necessary for the expression of *Ambn*. Our data suggest that NT-4 is also required for a high level of the expression of *Ambn*. We showed that NT-4 did not have an effect on the expression of *Runx2* in the dental epithelium (supplemental Fig. 2). Further, K252a treatment also did not cause any differences in *Runx2* or Sp3 expressions. Thus, neurotrophic factor signaling is not required to regulate the expression of *Runx2* and Sp3. The ERK-MAPK pathway provides a major link between the cell surface and nucleus to control proliferation and differentiation. The inhibition of MAPK signaling blocks osteoblast-specific gene expression in mature osteoblasts, whereas a constitutive active form of the MAPK intermediate, MEK1, is stimulatory (36). *Runx2* is required for cells to respond to MAPK *in vitro* (37). FGF2 induces osteocalcin expression through MAPK activation in osteoblast cell line and bone marrow stromal cells (40). We demonstrated that in the dental epithelium, ERK phosphorylation was induced by NT-4 and necessary for the phosphorylation of *Ambn* expression. In fact, the MEK inhibitor PD98059 inhibited ERK phosphorylation and *Ambn* expression in dental epithelium (data not shown). These results suggest that NT-4-*TrkB*-ERK signaling is important for *Ambn* expression and ameloblast differentiation.

## REFERENCES

- Thesleff, I., Vaahtokari, A., and Partanen, A. M. (1995) *Int. J. Dev. Biol.* **39**, 35–50
- Zeichner-David, M., Diekwisch, T., Fincham, A., Lau, E., MacDougall, M., Moradian-Oldak, J., Simmer, J., Snead, M., and Slavkin, H. C. (1995) *Int. J. Dev. Biol.* **39**, 69–92
- Fukumoto, S., and Yamada, Y. (2005) *Connect. Tissue Res.* **46**, 220–226
- Fukumoto, S., Miner, J. H., Ida, H., Fukumoto, E., Yuasa, K., Miyazaki, H., Hoffman, M. P., and Yamada, Y. (2006) *J. Biol. Chem.* **281**, 5008–5016
- Smith, C. E. (1998) *Crit. Rev. Oral Biol. Med.* **9**, 128–161
- Fukumoto, S., Kiba, T., Hall, B., Iehara, N., Nakamura, T., Longenecker, G., Krebsbach, P. H., Nanci, A., Kulkarni, A. B., and Yamada, Y. (2004) *J. Cell Biol.* **167**, 973–983
- Barbacid, M. (1994) *J. Neurobiol.* **25**, 1386–1403
- Barbacid, M. (1995) *Curr. Opin. Cell Biol.* **7**, 148–155
- Klein, R., Conway, D., Parada, L. F., and Barbacid, M. (1990) *Cell* **61**, 647–656
- Middlemas, D. S., Lindberg, R. A., and Hunter, T. (1991) *Mol. Cell Biol.* **11**, 143–153
- Tsoufias, P., Soppet, D., Escandon, E., Tessarollo, L., Mendoza-Ramirez, J. L., Rosenthal, A., Nikolics, K., and Parada, L. F. (1993) *Neuron* **10**, 975–990
- Valenzuela, D. M., Maisonpierre, P. C., Glass, D. J., Rojas, E., Nunez, L., Kong, Y., Gies, D. R., Stitt, T. N., Ip, N. Y., and Yancopoulos, G. D. (1993) *Neuron* **10**, 963–974
- Verdi, J. M., Birren, S. J., Ibanez, C. F., Persson, H., Kaplan, D. R., Benedetti, M., Chao, M. V., and Anderson, D. J. (1994) *Neuron* **12**, 733–745
- Mahadeo, D., Kaplan, L., Chao, M. V., and Hempstead, B. L. (1994) *J. Biol. Chem.* **269**, 6884–6891
- Di Marco, E., Mather, M., Bondanza, S., Cutuli, N., Marchisio, P. C., Cancedda, R., and De Luca, M. (1993) *J. Biol. Chem.* **268**, 22838–22846
- Kalcheim, C., Carmeli, C., and Rosenthal, A. (1992) *Proc. Natl. Acad. Sci. U. S. A.* **89**, 1661–1665
- Sariola, H., Saarma, M., Sainio, K., Arumae, U., Palgi, J., Vaahtokari, A., Thesleff, I., and Karavanov, A. (1991) *Science* **254**, 571–573
- Rabizadeh, S., Oh, J., Zhong, L. T., Yang, J., Bitler, C. M., Butcher, L. L., and Bredesen, D. E. (1993) *Science* **261**, 345–348
- Barrett, G. L., and Bartlett, P. F. (1994) *Proc. Natl. Acad. Sci. U. S. A.* **91**, 6501–6505
- Luukko, K., Arumae, U., Karavanov, A., Moshnyakov, M., Sainio, K., Sariola, H., Saarma, M., and Thesleff, I. (1997) *Dev. Dyn.* **210**, 117–129
- Nosrat, C. A., Fried, K., Lindskog, S., and Olson, L. (1997) *Cell Tissue Res.* **290**, 569–580
- Yuasa, K., Fukumoto, S., Kamasaki, Y., Yamada, A., Fukumoto, E., Kanaoka, K., Saito, K., Harada, H., Arikawa-Hirasawa, E., Miyagoe-Suzuki, Y., Takeda, S., Okamoto, K., Kato, Y., and Fujiwara, T. (2004) *J. Biol. Chem.* **279**, 10286–10292
- von Schack, D., Casademunt, E., Schweigreiter, R., Meyer, M., Bibel, M., and Dechant, G. (2001) *Nat. Neurosci.* **4**, 977–978
- Klein, R., Smeyne, R. J., Wurst, W., Long, L. K., Auerbach, B. A., Joyner, A. L., and Barbacid, M. (1993) *Cell* **75**, 113–122
- Conover, J. C., Erickson, J. T., Katz, D. M., Bianchi, L. M., Poueymirou, W. T., McClain, J., Pan, L., Helgren, M., Ip, N. Y., Boland, P., Friedman, B., Wiegand, S., Vejsada, R., Kato, A. C., Dechiara, T. H., and Yancopoulos, G. D. (1995) *Nature* **375**, 235–238
- Liu, X., Ernfor, P., Wu, H., and Jaenisch, R. (1995) *Nature* **375**, 238–241
- Ernfor, P., Lee, K. F., and Jaenisch, R. (1994) *Nature* **368**, 147–150
- Korte, M., Carroll, P., Wolf, E., Brem, G., Thoenen, H., and Bonhoeffer, T. (1995) *Proc. Natl. Acad. Sci. U. S. A.* **92**, 8856–8860
- Eide, F. F., Vining, E. R., Eide, B. L., Zang, K., Wang, X. Y., and Reichardt, L. F. (1996) *J. Neurosci.* **16**, 3123–3129
- Li, Y. X., Xu, Y., Ju, D., Lester, H. A., Davidson, N., and Schuman, E. M. (1998) *Proc. Natl. Acad. Sci. U. S. A.* **95**, 10884–10889
- Rose, C. R., Blum, R., Pichler, B., Lepier, A., Kafitz, K. W., and Konnerth, A. (2003) *Nature* **426**, 74–78
- Luukko, K., Moshnyakov, M., Sainio, K., Saarma, M., Sariola, H., and Thesleff, I. (1996) *Dev. Dyn.* **206**, 87–99
- Dhamija, S., and Krebsbach, P. H. (2001) *J. Biol. Chem.* **276**, 35159–35164
- Bouwman, P., Gollner, H., Elsasser, H. P., Eckhoff, G., Karis, A., Grosveld, F., Philippen, S., and Suske, G. (2000) *EMBO J.* **19**, 655–661
- Gollner, H., Dani, C., Phillips, B., Philippen, S., and Suske, G. (2001) *Mech. Dev.* **106**, 77–83
- Xiao, G., Gopalakrishnan, R., Jiang, D., Reith, E., Benson, M. D., and Franceschi, R. T. (2002) *J. Bone Miner. Res.* **17**, 101–110
- Ducy, P., Zhang, R., Geoffroy, V., Ridall, A. L., and Karsenty, G. (1997) *Cell* **89**, 747–754
- Xiao, G., Jiang, D., Thomas, P., Benson, M. D., Guan, K., Karsenty, G., and Franceschi, R. T. (2000) *J. Biol. Chem.* **275**, 4453–4459
- Franceschi, R. T., Xiao, G., Jiang, D., Gopalakrishnan, R., Yang, S., and Reith, E. (2003) *Connect. Tissue Res.* **44**, Suppl. 1, 109–116
- Xiao, G., Jiang, D., Gopalakrishnan, R., and Franceschi, R. T. (2002) *J. Biol. Chem.* **277**, 36181–36187

## Collagen type I matrix affects molecular and cellular behavior of purified porcine dental follicle cells

S. Tsuchiya · M. J. Honda · Y. Shinohara · M. Saito · M. Ueda

Received: 13 April 2007 / Accepted: 1 October 2007 / Published online: 13 November 2007  
© Springer-Verlag 2007

**Abstract** We investigated porcine dental follicle cells at the early crown-formation stage and examined the behavior of cells grown in a collagen type I (Col-I) matrix. Clone-porcine dental follicle cells (DFC-I) and controls, viz., dental follicle itself, nonclone-dental follicle cells, periodontal ligament cells (PDLC), and bone marrow stromal cells, were obtained from 6-month-old pigs. DFC-I showed a different gene expression pattern from controls by reverse-transcription polymerase chain reaction analysis. In addition, Col-I treatment enhanced DFC-I proliferation and increased their alkaline phosphatase activity compared with nontreated DFC-I. The expression of periostin, biglycan, and osteocalcin (OCN) in cells growing on collagen was upregulated, similar to the pattern seen in PDLC. DFC-I with and without Col-I treatment were combined with  $\beta$ -tricalcium phosphate particles and

implanted into immunodeficient mice. Significant differences were found in the gene expression patterns of bone sialoprotein, OCN, and periostin in both treated and nontreated implants at 2 and/or 4 weeks. The results showed that Col-I induced the mineralization pathway in these cells. Hard tissue formation was observed in both implant types at 8 weeks. Our results suggest that Col-I facilitates the differentiation of DFC-I along the mineralization process.

**Keywords** Characterization · Clonal dental follicle cell · Collagen type I matrix · Dental follicle · Mineralization · Porcine

### Introduction

The dental follicle (DF) is a loose, ectomesenchymally derived, connective tissue surrounding the enamel organ and the dental papilla of the developing tooth germ prior to eruption. The differentiation and function of dental follicle cells (DFC) are controlled by a network of regulatory molecules, including growth factors and cytokines (Thesleff and Mikkola 2002). Although the exact sequence of events and cells involved in the development of the periodontium is not established, previous studies have suggested that DFC populations also contain cementoblasts, periodontal ligament cells (PDLC), and osteoblast progenitor or precursor cells (Morszeck et al. 2005; Palmer and Lumsden 1987; Ten Cate and Mills 1972; Ten Cate et al. 1971; Yoshikawa and Kollar 1981). Bovine DFC isolated from developing tooth germ at the root-forming stage can differentiate into cementoblasts on implantation into immunodeficient mice (Handa et al. 2002). However, the mechanisms regulating DFC differentiation remain poorly understood (Bartold et al. 1988; Diekwisch 2001; Saygin et al. 2000).

This work was supported in part by grants from the Japanese Ministry of Education, Culture, Sports, Science, and Technology (Kakenhi Kiban B 16390578 and Houga 18659592 to M.J.H.) and by the Hitachi Medical Corporation (Japan) and DENICS International (Japan).

S. Tsuchiya · M. J. Honda (✉) · Y. Shinohara · M. Ueda  
Tooth Regeneration, The Division of Stem Cell Engineering,  
The Institute of Medical Science, The University of Tokyo,  
4-6-1 Shiroganedai, Minato-ku,  
Tokyo 108-8639, Japan  
e-mail: honda-m@ims.u-tokyo.ac.jp

S. Tsuchiya · M. Ueda  
Department of Oral and Maxillofacial Surgery,  
Nagoya University Postgraduate School of Medicine,  
65 Tsurumacho, Showa-ku, Nagoya,  
Aichi 466-8550, Japan

M. Saito  
Department of Operative Dentistry and Endodontics,  
Kanagawa Dental College,  
82 Inaokacho, Yokosuka,  
Kanagawa 238-8580, Japan

In the first part of this study, we isolated porcine DFC from third molars extracted at the early crown-formation stage. Using semiquantitative and real-time reverse-transcription polymerase chain reaction (sq-PCR and rt-PCR), we examined the expression of periodontal- and bone-related genes in these cells and compared them with the gene expressions of PDLC and bone marrow stromal cells (BMSC). The periodontal ligament (PDL) originates from DFC and contains heterogeneous cell populations (Lekic et al. 2001; Murakami et al. 2003). Recent findings suggest that PDLC have many osteoblast-like properties including the expression of bone-associated markers (Han and Amar 2003; Lekic et al. 2001; Marcopoulou et al. 2003; Ouyang et al. 2000; Pitaru et al. 2002). BMSC represent a population of nonhematopoietic marrow-derived cells, and their ability to differentiate into mesenchymal lineage includes osteoprogenitor cells (Bianco et al. 2001; Ducy et al. 1999). Recently, the skeletal site-specific characterization of orofacial BMSC was examined by Akintoye et al. (2006). Clone-porcine DFC (DFC-I) were derived from a single cell and were shown to adhere to a plastic substratum and to be clonogenic and competent to proliferate *in vitro*.

The extracellular matrix (ECM) relays complex signals from the cell microenvironment to direct proliferation and differentiation during tissue development. However, the role of the ECM and adhesion in DFC differentiation is poorly understood. BMSC undergo osteogenic differentiation *in vitro* when cultured on a collagen type I (Col-I) matrix (Mizuno and Kuboki 2001; Xiao et al. 1998). Moreover, Col-I also supports osteogenesis in BMSC and may induce differentiation in the absence of soluble osteoinductive factors (Klees et al. 2005; Salaszyk et al. 2004). Col-I is also a major organic component of the predentin-dentin matrix (Ruch 1998), and immature adult rat dental pulp cells strongly induces mRNA expression for dentin sialoprotein in Col-I gel cultures (Nakao et al. 2004). We have therefore hypothesized that Col-I might facilitate the differentiation of DFC. To test this, we cultured DFC on either dishes coated with purified Col-I (Col-I-d) or standard tissue-grade polystyrene dishes (P-d) and analyzed cell growth, alkaline phosphatase (ALPase) activity, and the expression of osteogenic differentiation-related marker genes. The gene expression patterns of Col-I-exposed DFC resembled that of PDLC. Periostin, biglycan, and osteocalcin (OCN) mRNAs were expressed, but bone sialoprotein (BSP) gene expression was absent.

As the final experiment in this study, we examined whether DFC-I could form hard tissue and assessed the effect of Col-I. The differentiated cells showed greater capacity to form hard tissue *in vivo* than the untreated cells. Our data presented herein provide new insights that Col-I affects the molecular and cellular behavior of purified porcine DFC.

## Materials and methods

### Isolation of highly purified DFC

As a preliminary experiment, mandibular third molar tooth buds were surgically removed from a 6-month-old porcine jaw and observed by histology and immunohistochemistry to establish the histogenesis (Fig. 1a–c). The DF and enamel organ were dissected as described previously (Wise et al. 1992). Briefly, the isolated DF was placed in 1% trypsin/1 mM EDTA (Invitrogen, Life Technologies, N.Y.) for 10 min at room temperature. The DF was separated from the dental enamel organ by microdissection and then incubated in 0.25% trypsin/1 mM EDTA (Invitrogen) for 10 min at 37°C to dissociate the porcine DFC. Approximately  $3.0 \times 10^6$  DFC were obtained from one tooth bud. The DFC were cultured in Dulbecco's modified Eagle's medium (DMEM; Kohjin Bio, Saitama, Japan) containing 10% fetal bovine serum (Invitrogen), 2 mM penicillin-streptomycin-glutamine (Invitrogen), and 1 mM sodium pyruvate (Invitrogen) at 37°C in an atmosphere containing 5% CO<sub>2</sub>. The medium was changed every 3 days until the third passage. DFC were then suspended at a density of 1 cell per 100  $\mu$ l and seeded into three 96-well culture plates (Greiner Bio-one, Kremsmuenster, Austria). The cells were incubated for 2 weeks, and then six colonies (each from a single cell) were observed and subsequently subcultured. For the following experiments, the clonal cell populations that had the greatest proliferation rate were subcultured until the tenth passage (DFC-I; Fig. 2a,b). The DFC-I were grown to a maximum of 30 passages.

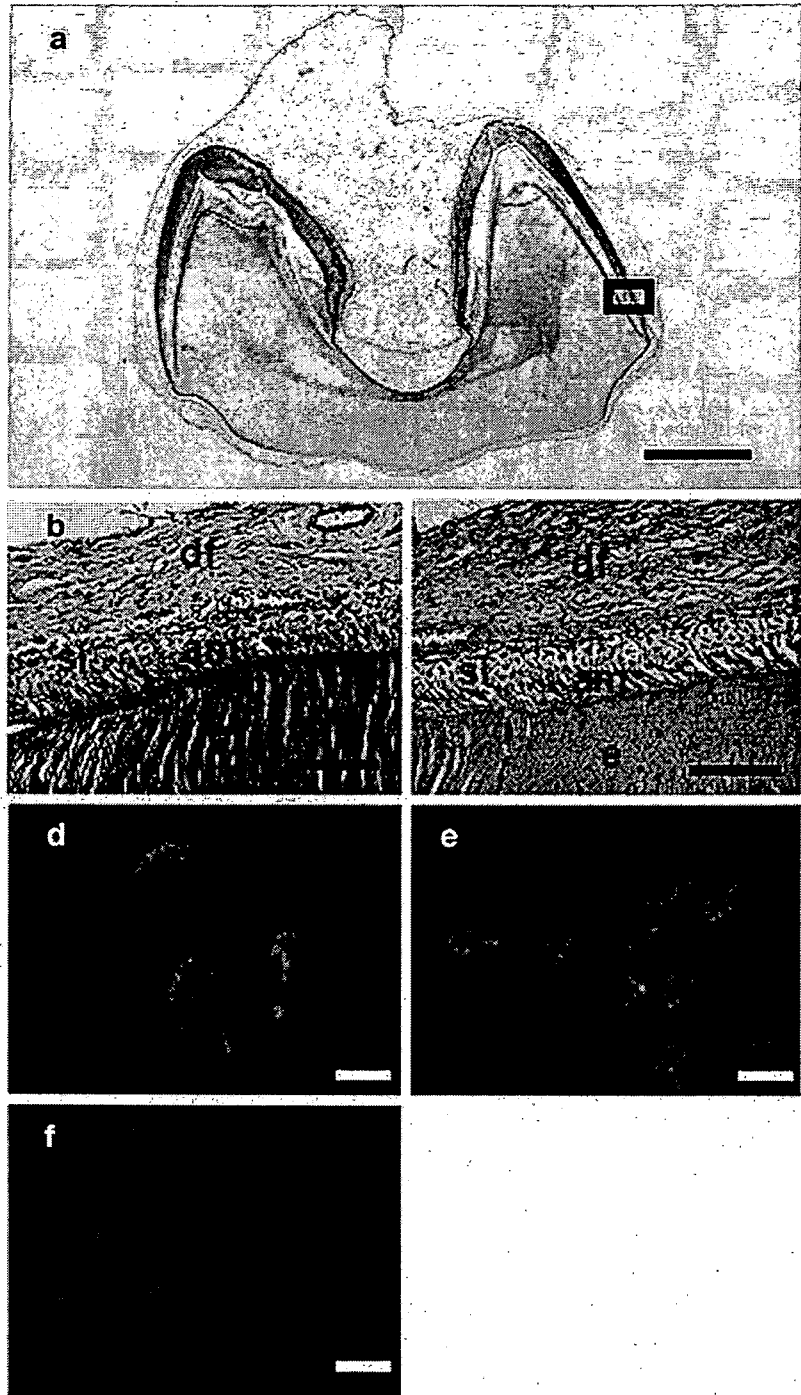
For comparison, cells were obtained from the PDL attached to the middle portion of the permanent incisor root and the alveolar bone surrounding the first molar tooth. These tissues were digested with 2 mg/ml collagenase (WAKO, Osaka, Japan), and the cells released were maintained as porcine PDLC (Fig. 2c,d) and porcine BMSC (Fig. 2e,f), respectively. The PDLC and BMSC at the third passages were used for following experiments.

### Immunofluorescent staining

We tested whether the DFC-I were derived from the DF by using mesenchyme markers. DFC-I grown on coverslips were fixed with 4% paraformaldehyde for 10 min at room temperature and then treated with 0.5% Triton-X 100 (Sigma, St. Louis, Mo.) for 5 min to render them permeable. After the blocking of non-specific sites, the cells were treated for 60 min with sheep antibody to pig Col-I (gift from Dr. J. Sodek, University of Toronto, Canada) diluted 1:20 with phosphate-buffered saline (PBS), with mouse antibody to vimentin (NeoMarkers, Westinghouse, Calif.) diluted 1:1,000, or with an antibody to cytokeratin14 as a control



**Fig. 1** Morphology of tissue and cells in porcine third molar at the crown-formation stage. **a** Morphology of third molar at the crown-formation stage shown by hematoxylin-eosin staining. Crown formation was well advanced at this stage. **b** Higher magnification of boxed area in **a** showing dental follicle (DF; *df*) distinguishable from the dental enamel organ and enamel (*e*). DF fibers were observed running close to the stratum intermedium (*si*) and contained fibroblastic cells (*am* ameloblast); hematoxylin-eosin staining. **c** Strong staining of collagen type I (Col-I) was identified in DF, but not in enamel or in enamel organ. **d, e** Immunofluorescence showed strong staining of all clone-porcine dental follicle cells (DFC-I) with specific antibody against vimentin and Col-I, respectively (blue DAPI nuclear staining). **f** DFC-I showed no staining with the specific antibody against cytokeratin14. Bars 1,000  $\mu\text{m}$  (**a**), 100  $\mu\text{m}$  (**b, c**), 10  $\mu\text{m}$  (**d–f**)



(1:100 dilution, Chemicon International, Calif.). Rhodamine-conjugated pig anti-rabbit IgG (DakoCytomation, Glostrup, Denmark) and pig anti-sheep IgG (Eappel, Biochemical Division, Auroa, Ohio), both diluted 1:200, were then applied for 60 min at room temperature. The stained cells were mounted and sealed with a PBS-glycerol mixture (1:9 v/v) containing DAPI (4,6-diamidino-2-phenylindole)

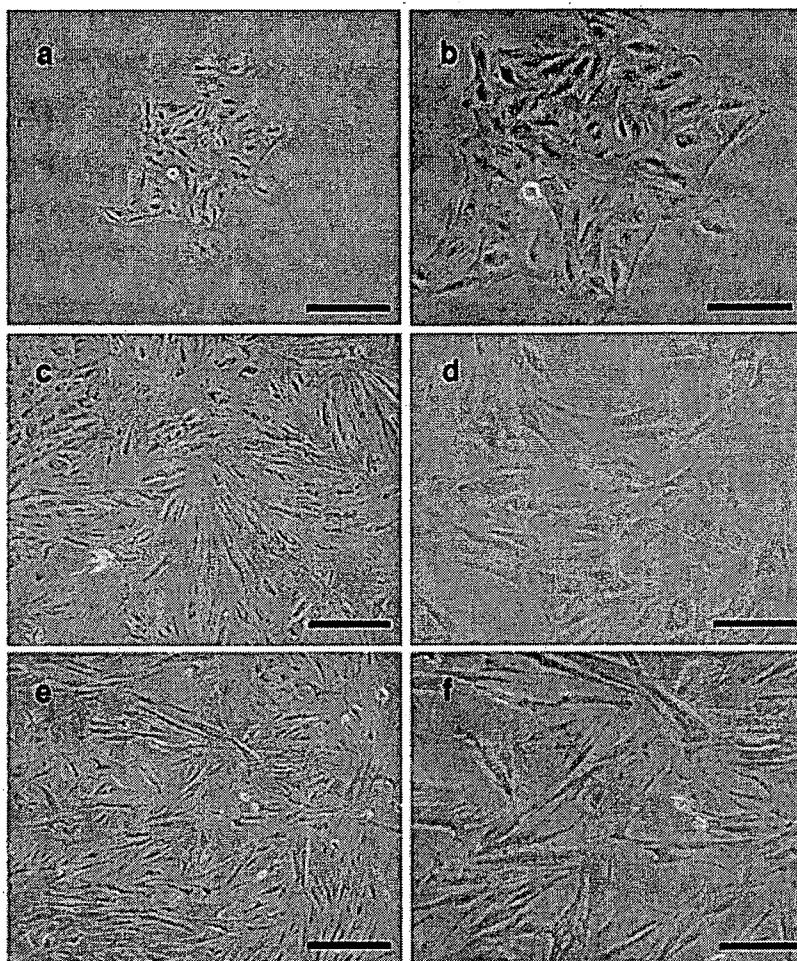
diluted 1:2,000. Non-immune sera of sheep and rabbit were used instead of primary antibodies as a control.

#### RNA preparation

Total RNA was isolated, by using TRIZOL REAGENT (Invitrogen Life Technologies) according to the manufac-



**Fig. 2** Cell morphology by phase-contrast microscopy. **a** At culture day 14, DFC-I formed small colonies. **b** Higher magnification of **a** showing the polygonal appearance of the cells at passage 1. **c** At culture day 7, periodontal ligament cells (PDLC) at passage 3 showed a fibroblastic morphology. **d** Higher magnification of **c** showing either spindle- or polygonal-shaped PDLC. **e** At culture day 7, bone marrow stromal cells (BMSC) at passage 3 were more fibroblastic in morphology than the PDLC. **f** At higher magnification, BMSC were either spindle or polygonal in shape. Bars 100  $\mu\text{m}$  (a, c, e), 50  $\mu\text{m}$  (b, d, f)



turer's instructions, from the DF at the early crown-formation stage, DFC at the 10th passage, DFC-I at the 10th passage cultured on P-d and Col-I-d, PDLC, BMSC, and implants at 1, 2, and 4 weeks after transplantation.

#### RNA analyses

cDNA were synthesized from 1  $\mu\text{g}$  total RNA in a 20- $\mu\text{l}$  reaction containing 10 $\times$  reaction buffer, 5 mM dNTP mixture, 1 U/ $\mu\text{l}$  RNase inhibitor, 0.25 U/ $\mu\text{l}$  reverse transcriptase (M-MLV reverse transcriptase, Invitrogen), and 0.125  $\mu\text{M}$  random primers (Takara, Tokyo, Japan). For sq-PCR, amplification was performed in a PCR Thermal Cycler SP (Takara) for 25–35 cycles according to the following reaction profile: 95°C for 30 s, 45–60°C for 30 s, and 72°C for 30 s. Porcine glyceraldehyde-3-phosphate dehydrogenase (GAPDH) primers were used as internal standards. The percentage of mRNA expression in the implants from the in vivo gene expression analysis was measured by using Scion Image picture-imaging software (Scion, Frederick, Md.). Synthesized cDNA served as a

template for subsequent PCR amplification with specific primers as listed in Table 1.

Real-time PCR was performed to quantify absolute mRNA expression by using the ABI PRISM 7900HT (Applied Biosystems, CA) with Absolute QPCR SYBR Green Mixes (Applied Biosystems). Primers were designed by using Primer-Express software (Applied Biosystems); the sequences are listed in Table 2. The thermocycling parameters were optimized at 50°C for 2 min, 95°C for 15 min, and 40 cycles of 95°C for 15 s and 61°C for 1 min. Cycle threshold (Ct) values were determined and employed to calculate relative gene amounts. The specificity of the PCR products was evaluated from the melt temperature ( $T_m$ ) of the PCR products by using dissociation curve analysis. PCR products were quantified by means of Microsoft Excel (Microsoft, Wash.) to compare the amplification of the target genes with that of GAPDH as a reference gene, with calibrator normalization and amplification efficiency correction. All experiments were repeated three times, and significant statistical differences were determined by Student's *t*-test ( $P < 0.05$ ).

**Table 1** Sequences of primer pairs used for reverse-transcription polymerase chain reaction (*CTGF* connective tissue growth factor, *GAPDH* glyceraldehyde-3-phosphate dehydrogenase)

Gene	Sequence	Annealing temperature (°C)	Products (bp)	Accession number or reference
Collagen type I	Forward 5'-GATCCTGCTGACGTGGCCAT Reverse 5'-ACTCGTGACGCCGTCGTAGA	55	212	AY350905
Collagen type III	Forward 5'-TCCCCAGCAAAAGATTTCAC Reverse 5'-AGCACCATTGAGACATTTGAA	45	237	AJ289758
Bone sialoprotein	Forward 5'-ACTGAAGCCCAAGGAACCAC Reverse 5'-TCCAACGTGGTCTTCTGGAC	48	480	L10363
Runx2/cbfa1	Forward 5'-GACCCTGGAAGGAAACACAA Reverse 5'-CGCTGGTCCATGCTTAGAGT	56	303	Iohara et al. 2004
Osteocalcin	Forward 5'-TCAACCCCGACGACGAG Reverse 5'-GACCGTCGACRAAACCCCTGA	60	204	AY150038
Osteopontin	Forward 5'-GCAATGAGCATTCCAATGTG Reverse 5'-GACCGTCGACTAAACCCTGA	56	383	X16575
Periostin	Forward 5'-CTGCACATGCAAGGATGACT Reverse 5'-ACATGGAGTTTCCCAGGCTA	54	589	AY880669
Biglycan	Forward 5'-GATGGCCTGAAGCTCAA Reverse 5'-GGTTGTTGAAGAGGCTG	60	406	AF159382
CTGF	Forward 5'-GCTCTTCTTCATGACCTCACCGT Reverse 5'-GCGGCTTACCGACTGGAAGACAC	60	411	U70060
GAPDH	Forward 5'-TCGACCACAGGGTAGGTTTC Reverse 5'-CCCAGCATCAAAGGTAGAA	45	497	AF017079

#### Measurement of cell proliferation

DFC-I were plated at a density of  $5 \times 10^3$  cells/ml into 6-well Col-I-d and standard tissue-grade P-d (BD Biosciences, Mountain View, Calif.). The DFC-I in each well were counted by using a WST-8 kit (Cell-counting Kit-8; Dojindo Laboratories, Kumamoto, Japan). The counting technique employed a tetrazolium salt that produces a highly water-soluble formazan dye. After a 1-h incubation with reagent according to the manufacturer's instructions, the relative cell

number was determined by measuring the absorbance of light at a wavelength of 450 nm at days 1, 7, and 14 (Model 650 Microplate Reader, Biorad Laboratories, Hercules, Calif.).

#### Assay for ALPase activity

DFC-I were plated at density of  $5 \times 10^3$  cells/ml into 6-well Col-I-d and P-d (BD Biosciences). For quantitative analysis of ALPase activity, *p*-nitrophenol production was measured at 37°C for 6 min in Milli-Q water by using a Fast *p*-

**Table 2** Sequence of primer pairs for real-time polymerase chain reaction (*GAPDH* glyceraldehyde-3-phosphate dehydrogenase)

Gene	Sequence	Annealing temperature (°C)	Products (bp)	Accession number
Collagen type I	Forward 5'-TCAAAGTCTTCTGCAACATGGAG Reverse 5'-GGCACGCTGGGCTGAG	61	79	AY350905
Collagen type III	Forward 5'-TTGGCCCTGTTTGCTTTTATAA Reverse 5'-CAAAAGGAACACATATGGAGTGTGA	61	82	AJ289758
Bone sialoprotein	Forward 5'-CCGAGGCCGAGAATATCACTC Reverse 5'-TTCCCGGCGTTACGTCC	61	66	L10363
Osteocalcin	Forward 5'-CTGGCTGATCACATCGGCT Reverse 5'-GCGAGGTCTAGGCTATGCCAT	61	64	AY150038
Osteopontin	Forward 5'-GCTGTCCCCACGGGAGA Reverse 5'-TTTGTACCTCAGTCCATAGACCAC	61	66	X166575
Periostin	Forward 5'-GGTCACAGACGTGGATTGGAT Reverse 5'-CCAGTTGGAGCTGTAGCCACT	61	71	AY880669
Biglycan	Forward 5'-AACGGGAGCCTGAGTTTTCTG Reverse 5'-CACCTGGACAGCTTGTGTT	61	69	AF159382
GAPDH	Forward 5'-GGGTCATCATCTCTGCCCT Reverse 5'-CTCATGGTTACGCCCCACT	61	68	AF017079

nitrophenyl phosphate tablet set (Sigma) as a substrate. The relative amount of *p*-nitrophenol was estimated from the light absorbance at a wavelength of 405 nm at days 1, 7, and 14 (Bio-Rad Laboratories).

#### In vivo differentiation assay

The differentiation potential of individual DFC-I on transplantation into immunodeficient mice was assessed as described previously (Handa et al. 2002). Briefly,  $1.5 \times 10^6$  DFC-I were incubated in a mixture of 40 mg  $\beta$ -tricalcium phosphate powder (TCP; Osferion G1, no. BH064005, Olympus Biomaterials, Tokyo, Japan) and fibrin clot (mixture of mouse fibrinogen and thrombin; both from Sigma) and were then inoculated subcutaneously into 5-week-old female CB-17 scid/scid (scid; severe combined immunodeficiency) mice (Nihoncrea, Tokyo, Japan). Mice were sacrificed after 1, 2, 4, and 8 weeks. The implants removed at 1, 2, and 4 weeks after transplantation were cut in half for histochemical analysis, calcification analysis, and mRNA expression analysis of periodontium matrix components. The implants removed at 8 weeks after transplantation were only used for histological analysis.

At 4 and 8 weeks after transplantation, the implants were fixed, decalcified with 10% EDTA-2Na, and then processed

for histological examination by using standard procedures. Sections were stained with hematoxylin-eosin for histological observation and prepared for immunohistochemistry.

Immunohistochemical analysis was performed by using the Vectastain ABC kit (Vector Laboratories), as previously described (Hsu et al. 1981) with modification (Chen et al. 1991a). The antibody used was an affinity-purified rabbit anti-pig BSP polyclonal antibody (gift from Dr. J. Sodek, University of Toronto, Canada) (1:2,000 dilution). To determine the potential for hard tissue formation in the DFC-I, we selected 15 sections at random from at least five specimens.

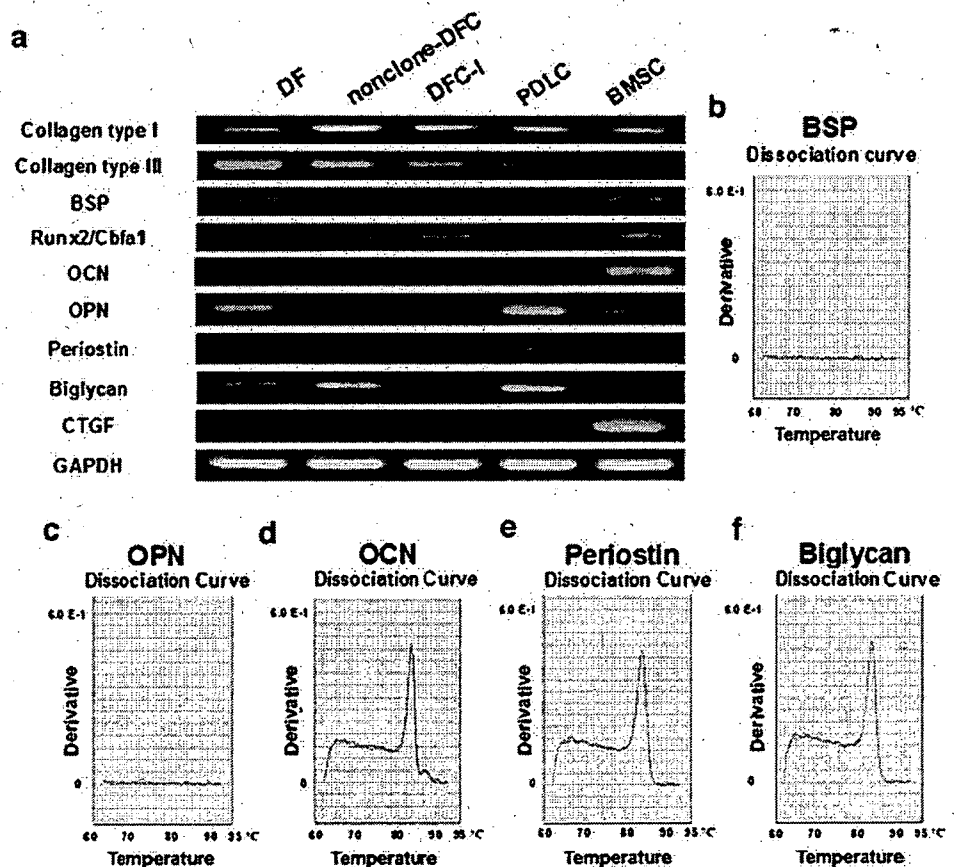
The Von Kossa staining procedure was also performed to analyze the extent of calcification in hard tissue, as described previously (Piattelli et al. 1994).

## Results

### Porcine third molar at early crown-formation stage

The 6-month porcine third molar appeared at the crown-formation stage (Fig. 1a), with the formation of hard tissues being well advanced. The DF was clearly distinguished from the dental enamel organ and enamel at high magnifi-

**Fig. 3** a Semiquantitative RT-PCR analysis of osteoblast-lineage/periodontal ligament-related genes in DF, nonclone-DFC, DFC-I, PDLC, and BMSC. In DFC-I, there was no detectable expression of mature cementoblast/osteoblast markers such as bone sialoprotein (*BSP*), osteopontin (*OPN*), osteocalcin (*OCN*), connective tissue growth factor (*CTGF*), and biglycan, and no periostin. The expression of *OPN*, biglycan, and *BMP-4* was higher in PDLC than in BMSC, but *Runx2/Cbfa1*, *CTGF*, and *ALPase* showed lower expression in PDLC than in BMSC. b–f Melting profile of the amplicon of *BSP*, *OPN*, *OCN*, periostin, and biglycan in DFC-I by real-time RT-PCR. Results were obtained by using the Sequence Detection Systems of dissociation curve software. *OCN*, periostin, and biglycan expressions were detected in DFC-I, but *BSP* and *OPN* were not detected



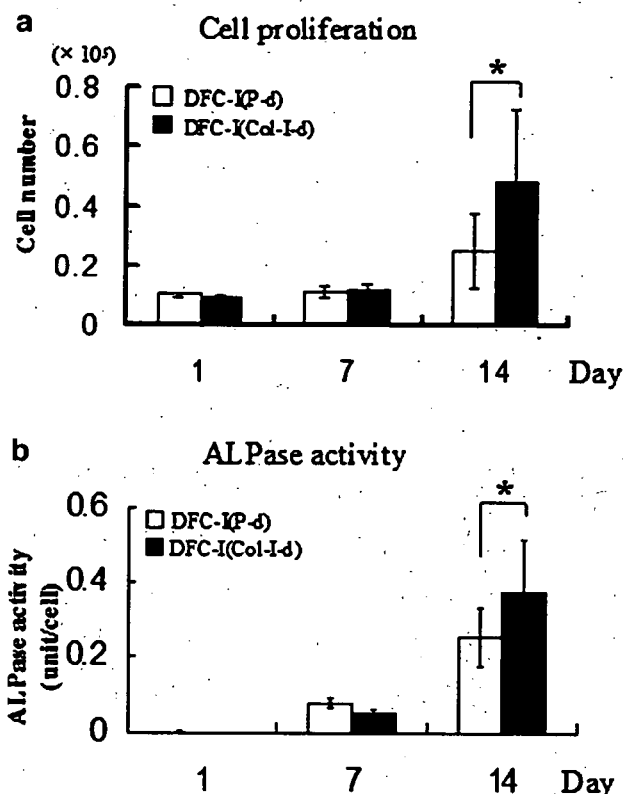


**Fig. 4** Effects of Col-I matrix on DFC-I on cell proliferation (a) and ALPase activity (b). The cells were seeded at a density of  $5.0 \times 10^3$  cells in standard 6-well plates (P-d) or in 6-well plates coated by Col-I (Col-I-d). No significant differences were apparent at 1 and 7 days. At 14 days, cell proliferation and ALPase activity of DFC-I cultured on Col-I-d were significantly higher than those on P-d. \*Statistically significant at  $P < 0.05$  (paired *t*-test)

cation by the increased collagen fibrils occupying the extracellular spaces between the follicular fibroblasts (Fig. 1b). ECM in the DF was positive for the Col-I mesenchymal marker by immunohistochemistry (Fig. 1c).

**Immunofluorescent staining of DFC**

Immunofluorescent staining was then carried out to determine the lineage of the isolated cells by using antibodies specific for vimentin (Fig. 1d) and Col-I (Fig. 1e) as mesenchymal markers, and an anti-cytokeratin14 antibody as an epithelial marker (Fig. 1f). All isolated cells were positive for Col-I and vimentin and negative for cytokeratin14 (nuclei showed blue DAPI staining). These results demonstrated that all isolated cells were derived from mesenchyme with no contamination from dental epithelial cells.

**Purification of DFC**

One DFC-I colony was expanded and analyzed over a number of weeks in culture, producing a cumulative expansion in

the single cell clones for over 30 passages prior to the onset of cellular senescence. Overall, six clones were expanded; the other clones exhibited only moderate growth potential that did not persist beyond 20 passages. The DFC-I comprised polygonal cells (Fig. 2a,b), whereas both the PDLC (Fig. 2c,d) and BMSC (Fig. 2e,f) had a mixed morphology including spindle-shaped and polygonal-shaped cells.

**Gene expression pattern of DFC-I**

We surveyed gene expression patterns in the DF, nonclone-DFC, DFC-I, PDLC, and BMSC by sq-PCR analysis (Fig. 3a). A series of genes are known to be involved in the morphogenesis of periodontium and bone (Table 1). The expression patterns of three DF-related genes in the DF, nonclone-DFC, and DFC-I were markedly different. mRNA expression for BSP and osteopontin (OPN) was only detected in the DF. Biglycan was expressed only in the DF and nonclone-DFC. From these results, the expression pattern of DFC-I resembled the more immature stage. Differences were also found when we compared the gene expression profiles of DFC-I, PDLC, and BMSC. BSP, OCN, and connective tissue growth factor (CTGF) expression was detected only in BMSC, whereas OPN, periostin, and biglycan were expressed only in the PDLC and BMSC. Runx2/Cbfa1 mRNA was expressed in all cell types. The expression levels of GAPDH were consistent across samples. BSP, OCN, OPN, periostin, and biglycan were not detected in DFC-I. by sq-PCR, prompting further investigation by rt-PCR for these genes (Table 2). Surprisingly, cementoblast/osteoblast markers such as BSP and OPN were not detected in DFC-I, but periostin, biglycan,

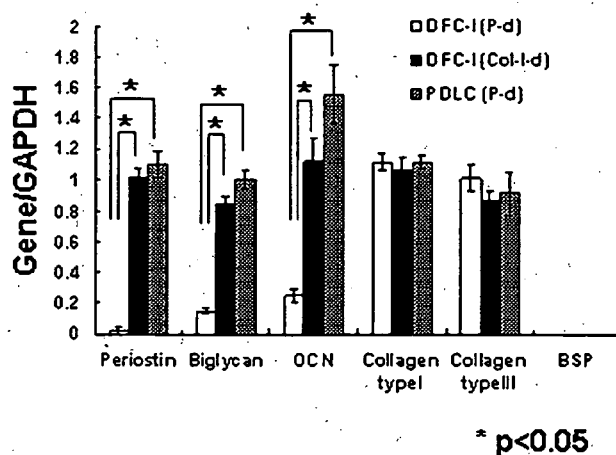


**Fig. 5** Effects of Col-I matrix on mRNA expressions in DFC-I cultured on P-d and Col-d and in PDLC on P-d as measured by using real-time RT-PCR. DFC-I cultured on Col-I-d showed upregulated gene expression of periostin, biglycan, and OCN, whereas BSP were not expressed in any of the three cell classes. The results were consistent within three independent experiments. \*Statistically significant at  $P < 0.05$  (paired *t*-test)